RESEARCH PAPER

Numerical Investigation of Nailing Pattern Effect on Nailed Wall Performance

Shahir, H.[1]* and Delfan, S.[2]

[1] Associate Professor, Department of Civil Engineering, Faculty of Engineering, Kharazmi University, Tehran, Iran.
[2] M.Sc., Department of Civil Engineering, Faculty of Engineering, Kharazmi University, Tehran, Iran.

© University of Tehran 2021

ABSTRACT: In this paper, the performance of soil nailed walls with various nail patterns has been studied to find an optimum layout based on the deformation criterion. To this end, parametric analysis on soil nailed walls with various nailing patterns is performed. Nine patterns including one uniform and eight variable nails length are considered. For each pattern, parametric analysis on different parameters including wall height, surcharge, nails spacing is implemented to find an optimum pattern based on the deformation criterion. The simulation results indicate that using the variable layout with long nails at the top of the wall not only reduces the lateral deformation of soil nailed wall but also decreases the density of nails.

Keywords: Deformation, Finite Element, Optimum Pattern, Safety Factor, Soil Nailing.

1. Introduction

Soil nailing is a common method to stabilize excavated slopes and walls. Where buildings or underground facilities exist near the excavation, in addition to checking the overall stability, the amount of deformations shall also be evaluated to ensure the appropriate performance of the wall and nearby structure.

Deformation of soil nailed walls has been studied by various researchers using experimental or numerical approaches. Plumelle et al. (1990), Tei et al. (1998) and Chu and Yin (2005) studied the response of soil-nailed walls using full-scale and centrifuge experiments. Numerical modeling has been successfully applied to model the behavior of soil nailed walls and slopes (Unterreiner et al., 1997; Seo et al., 2014; Ardakani et al., 2014; Liu et al., 2016; Moniuddin et al., 2016; Rawat and Gupta, 2016; Hitha et al., 2019; Rashidi et al., 2019; Rashidi and Shahir, 2019; Gharedaghi and Shahir, 2019; Hajiazizi and Mirzazadeh, 2020; Abbas et al., 2020). A verified numerical model makes it possible to study the effects of various parameters such as nails length and spacing.

The effects of spacing and length of nails on the performance of soil nailed wall have been studied by a few researchers. Fan and Luo (2008) performed numerical study on the optimal nails layout for various slope angles in terms of factor of safety using 2D finite element program. Their study showed

---

that the nails length at the lower 1/3 part of the slope has a significant impact on the overall stability, especially for soil nailed walls. They also concluded that the effect of vertical spacing of nails on the stability of soil nailed slopes is insignificant if the length and number of nails remain unchanged. Yang and Drumm (2000) using 3D finite element modeling, concluded that the short nails are not effective because the long term deformations occurs in the upper part of the soil nailed slope. Zhang et al. (1999) developed a 3D finite element model for the deformation analysis of soil nailed walls and investigated the effects of nail length and spacing on horizontal deflection. Uniform distribution of nails was considered. They indicated that the horizontal deflection decreases with increasing nails length and decreasing nails spacing.

In the previous studies, an inclusive study on the effect of the nailing arrangement on the wall deformation considering various wall heights and nail spacing and determination of the optimum pattern based on the deformation criterion have not been accomplished. Halabian et al. (2012) used a 3D numerical model to evaluate the earth pressure distribution during and after excavation. They also studied the effects of different crucial factors such as nail inclination, nail length, length pattern, slope inclination and nail bars arrangement on the performance of soil-nailed structures. The research implied that using nails with inclination angle varying in the range of 0 to 15 deg results in a reduction of lateral earth pressure. To study the effect of nails length and pattern, they assumed that nails are placed horizontally. The results showed that nails with longer length placed in the upper third part of the wall contribute more in the wall horizontal displacement reduction while nails with longer lengths placed in lower part of the wall provide more stability to the structure as well as reduction in horizontal displacements.

Sharma and Ramkrishnan (2020) studied potential parametric optimization in soil nailing. They considered reduced nail length pattern to study the possible optimization of nail length. Their study showed that the nail length for the lower-third portion could be reduced by 10-20% of their lengths than in the upper-third and middle-third portion of the wall.

To study the effects of pullout strength on horizontal displacement, uniform pattern and reduced nail length pattern were considered by the researchers. Their study showed that the middle third portion which is more susceptible to pull-out failure undergo maximum displacements and using reduced nail length pattern marginally increases the horizontal displacements. In the above mentioned studies, the effects of various nailing arrangements, nails spacing and wall height on the wall deformations have not been completely studied and only three patterns have been considered. Also, the effects of excavation-induced ground movements on the performance and serviceability of the adjacent buildings have not been studied.

In this study, nine patterns including one uniform and eight variable nails length have been considered. For each pattern, parametric analysis on different parameters including wall height, surcharge, nails spacing was done. The nailed walls were designed using limit equilibrium method according to recommendation procedure and safety factors in the nailing manual of FHWA (Lazarte et al., 2015), for temporary conditions. After determination of the required nails length, nailed wall deformations were predicted using the non-linear finite element analysis. To verify the employed model, a two-dimensional finite element analysis of a full-scale experimental soil nailed wall was performed and compared with the field measurements.

2. Description and Verification of the Numerical Model

To analyze the deformation of nailed walls,

the wall has been modeled in the plane strain condition. In the two-dimensional analysis, nails are modeled using the "equivalent plate" approach. In this method, the discrete nails are replaced by a continuous plate with the stiffness equal to the stiffness of the nail divided by the horizontal spacing. For the grouted nails, an equivalent modulus of elasticity (E_{eq}) can be determined as follow:

$$E_{eq} = E_n \left(\frac{A_n}{A}\right) + E_g \left(\frac{A_g}{A}\right) \qquad (1)$$

where E_n and E_g: are the elastic modulus of the bar and grout material, respectively. A: is the total cross-sectional area of grouted nails. A_n and A_g: are the cross-sectional area of bar and grout cover, respectively. It should be noted that due to the insignificant tensile strength of the grout, the effect of grout has been neglected in the calculation of equivalent EA. Also, the bending stiffness of nails is neglected. The axial stiffness of nails can be determined as follow:

$$EA(kN/m) = \frac{E_{eq}}{S_h} A \qquad (2)$$

where S_h: is the horizontal spacing of nails.

The hardening soil model (HS model) has been used to simulate the soil behavior. It is an advanced constitutive model that can be used for both soft and stiff soils. This model is able to simulate stress dependency of soil stiffness. Limit state of stress are described by means of the friction angle (ϕ) and cohesion (c). The soil stiffness is described using three moduli: the triaxial loading modulus, E_{50}, the triaxial unloading modulus, E_{ur} and the oedometer loading modulus, E_{oed}. The stress dependency of these three moduli is defined by the following equation:

$$E = E^{ref} \left(\frac{c \cos \phi + \sigma_3' \sin \phi}{c \cos \phi + p^{ref} \sin \phi}\right)^m \qquad (3)$$

where m: is the fabric parameter used to determine the amount of stress dependency of stiffness, E^{ref}: is the reference stiffness modulus corresponding to the reference confining pressure p^{ref}, and σ_3': is the confining pressure in a triaxial test. As a default, $p^{ref} = 100 \, kPa$ is used. Schanz and Vermeer (1998) indicated that E_{oed}^{ref} can be considered equal to E_{50}^{ref} for sand and gravel soils. As an average value for various soil types, E_{ur}^{ref} is assumed equal to $3E_{50}^{ref}$.

To verify the utilized numerical model, a full-scale test called Clouterre (FHWA, 1993; Plumelle et al., 1990; Unterreiner et al., 1997) was simulated. The French national project Clouterre was conducted from 1986 to 1991 to study the behavior of soil nailed walls during construction, in service and at failure. The schematic cross-section of the constructed soil-nailed wall in the Clouterre test is shown in Figure 1 (Unterreiner et al., 1997). The nailed wall is 7.3 m high and 7.5 m wide that is restricted between two lateral walls covered with a double layer of polyethylene sheet greased to ensure plane strain condition. The wall was constructed by excavation steps of 1 m height with the installation of nails at the horizontal spacing of 1.15 m. Hollow aluminum tubes with various diameter, thickness and length were used as nail elements in this test. Inclination of nails is 10 deg and their length range from 6 to 8 m. Each nail was fixed to 80 mm thick shotcrete facing. The facing, made of mesh-reinforced shotcrete, was installed after placing the nails. Properties of the nails and shotcrete facing used in the finite element analysis are listed in Tables 1 and 2.

Table 1. Properties of nails used in the simulation of Clouterre test

Parameter	Symbol	Unit	Type A	Type B	Type C
Tube thickness	e	mm	1	2	1
Tube diameter	φ	mm	16	30	40
Axial stiffness	EA	kN/m	2870	10700	7500
Yield force	N_p	kN/m	4.52	16.8	11.7

Table 2. Properties of shotcrete facing used in the simulation of Clouterre test

Parameter	Symbol	Unit	Value
Unit weight	γ	kN/m^3	24
Young's modulus	E	kPa	25×10^6
Axial stiffness	EA	kN/m	2×10^6
Bending stiffness	EI	$kN.m^2/m$	1067
Shotcrete thickness	d	m	0.08
Poisson ratio	ν	-	0.2
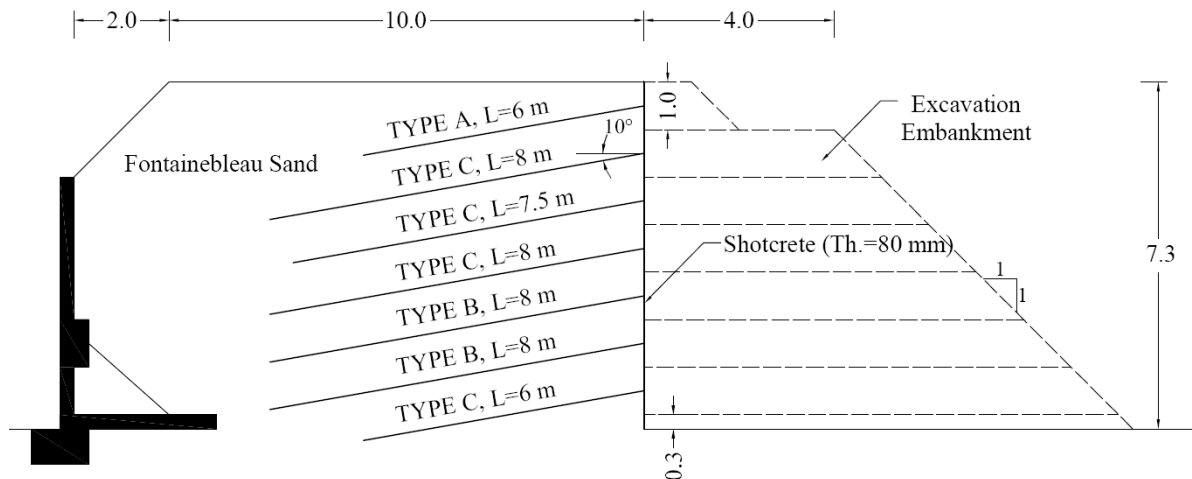
Fig. 1. Cross-section of the soil-nailed wall in the Clouterre test (Unterreiner et al., 1997)

In the Clouterre test, backfill and foundation soils are the Fontainebleau sand with different densities. The physical and mechanical properties of backfill and foundation soils were reported by Unterreiner et al. (1997) as presented in Table 3.

The stiffness parameters of the HS model can be evaluated based on the results of the conducted pressuremeter tests. The results of pressuremeter tests within the backfill soil before construction of the nailed wall (Plumelle et al., 1990; Unterreiner et al., 1997) are presented in Table 3. Unterreiner et al. (1997) compared the results of pressuremeter tests with the results of compression triaxial tests performed on the medium to dense Fontainebleau sand

samples by Dupla and Canou (1994). Their comparison showed that the ratio (α) of soil stiffness modulus (E) to the Menard pressuremeter modulus (E_M) varies from 2.2 to 2.8 with depth which is in agreement with the recommended values by Plumelle et al. (1990) and Unterreiner et al. (1997).

$$E_{soil} = \alpha \times E_M \qquad (4)$$

To obtain the parameters of the HS model, the values of soil stiffness at different depths have been calculated using the aforementioned ratio. By applying the following equation, E_{50}^{ref} and m can be determined by curve-fitting to the soil stiffness modulus as shown in Figure 2.

Table 3. Summary of calculations of the stiffness parameters of backfill soil

Depth (m)	E_M (MPa)	α	$E_{50}=\alpha. E_M$ (MPa)	σ_c (kPa)	β
1	7.0	2.2	15.4	9.5	0.13
2	6.5	2.3	15.0	19.0	0.22
3	11.0	2.4	26.4	28.5	0.31
4	12.0	2.5	30.0	38.0	0.40
5	10.5	2.6	27.3	47.5	0.49
6	14.5	2.7	39.2	57.0	0.59
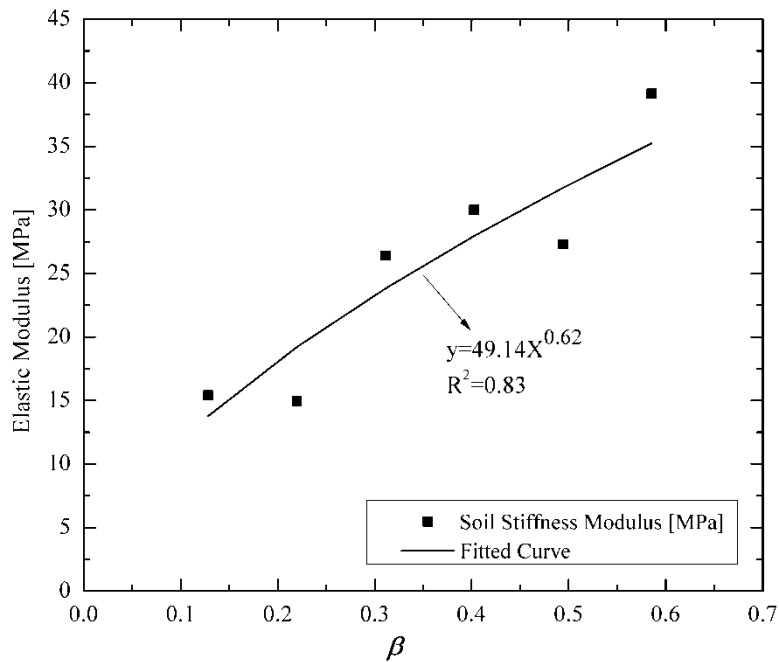
Fig. 2. Evaluation of stiffness parameters of backfill soil based on the pressuremeter results

$$E_{soil} = E_{50}$$
$$= E_{50}^{ref} (\frac{c \cos \phi + \sigma_3' \sin \phi}{c \cos \phi + p^{ref} \sin \phi})^m$$
$$= E_{50}^{ref} \times \beta^m \qquad (5)$$
$$\beta = \frac{c \cos \phi + \sigma_3' \sin \phi}{c \cos \phi + p^{ref} \sin \phi}$$

where c and φ: are the cohesion and friction angle of soil, respectively. σ_3': is the confining soil pressure which can be calculated by the following equation:

$$\sigma_3' = \sigma_v' \left(\frac{1 + 2k_0}{3}\right) \qquad (6)$$

where σ_v': is the vertical soil stress and k_0: is the coefficient of earth pressure at rest. A summary of calculations is presented in Table 3. As shown in Figure 2, the obtained values of E_{50}^{ref} and m from the best fitted curve are 49.1 MPa and 0.62, respectively.

Regarding the foundation soil, two pressuremeter tests were carried out by Schlosser et al. (1993) and the average pressuremeter modulus of the foundation soil in depth of 0 to 7 m was measured as 35 MPa. Therefore, the values of E_{50}^{ref} and m can be determined as above. The evaluated values of the foundation soils parameters are presented in Table 4.

The construction of Clouterre test was interrupted for two months between phases five and six. During the interruption significant creep movement was measured at the top of the wall. In this paper, the instantaneous deformations have been considered and the creep effect was not taken into account. Thus, the first five phases of excavation have been simulated and compared with the measured results. The finite element mesh of the Clouterre wall is shown in Figure 3.

In Figures 4 and 5, the simulation and measured results for the horizontal displacement in the wall height have been compared at the end of phases 3 and 5 where the excavation depths were 3 and 5 m, respectively. The results have also been compared with the results of finite element analysis of Unterreiner et al. (1997). They used the finite element code CESAR–LCPC and a finite element meshes with rectangular 8-node elements and non-associated Mohr–Coulomb constitutive model for both of the foundation and backfill soils.

As depicted in these figures, the simulation results are somewhat more than the measured values in both phases. Acceptable agreement is observed between the curves. It is notable that significant jump

in the measured lateral deformation is observed at the upper part of the wall, while it can be seen the more uniform trend in the predicted results.

Figure 6 shows the tensile force distribution in the nails length for the upper four rows at the end of phase 5. There is an

acceptable agreement between simulation results and numerical modeling results of Unterreiner et al. (1997). The maximum difference between two curves for nails No. 1, 3, and 4 is about 0.5 to 1.5 kN. For nail No. 2, this difference is about 3 kN.

Table 4. Parameters of the backfill and foundation soils for the HS model

| Parameter	Symbol	Unit	Backfill soil	Foundation soil
Cohesion	c	kPa	3	0
Friction angle	φ	deg	38	36
Dilation angle	ψ	deg	25	20
Unit weight	γ	kN/m^3	16.1	17.0
Reference loading stiffness	E_{50}^{ref}	kPa	4.91×10^4	1.72×10^4
Reference oedometer loading stiffness	E_{oed}^{ref}	kPa	4.91×10^4	1.72×10^4
Reference unloading stiffness	E_{ur}^{ref}	kPa	1.47×10^5	5.16×10^4
Reference confining pressure	P^{ref}	kPa	100	100
Poisson ratio	ν	-	0.39	0.37
Fabric parameter	m	-	0.62	0.62
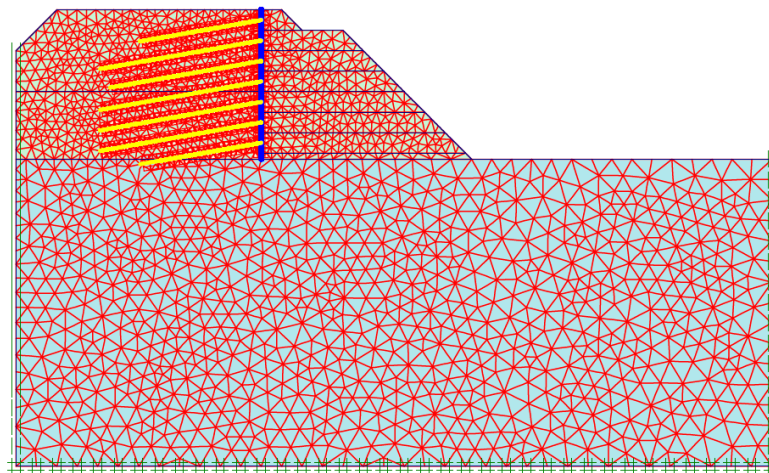
Fig. 3. Finite element mesh of the Clouterre test

(a)

(b)
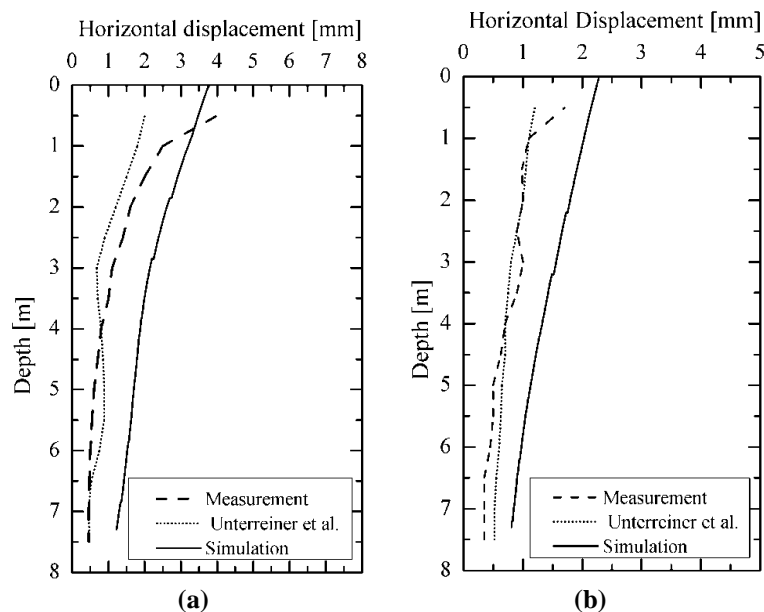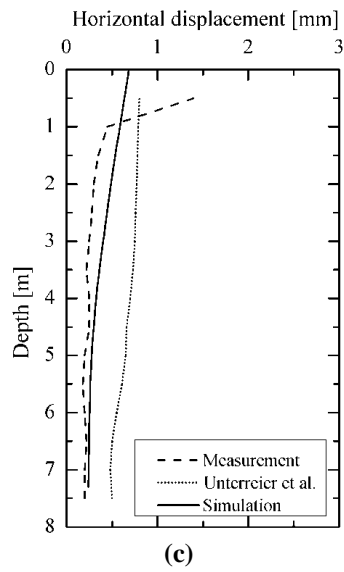
Fig. 4. Comparison of the predicted horizontal displacements in the backfill with measured results in phase 3 at: a) 2 m; b) 4 m; and c) 8 m behind the wall facing
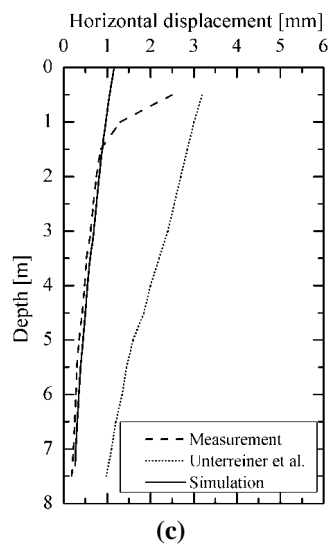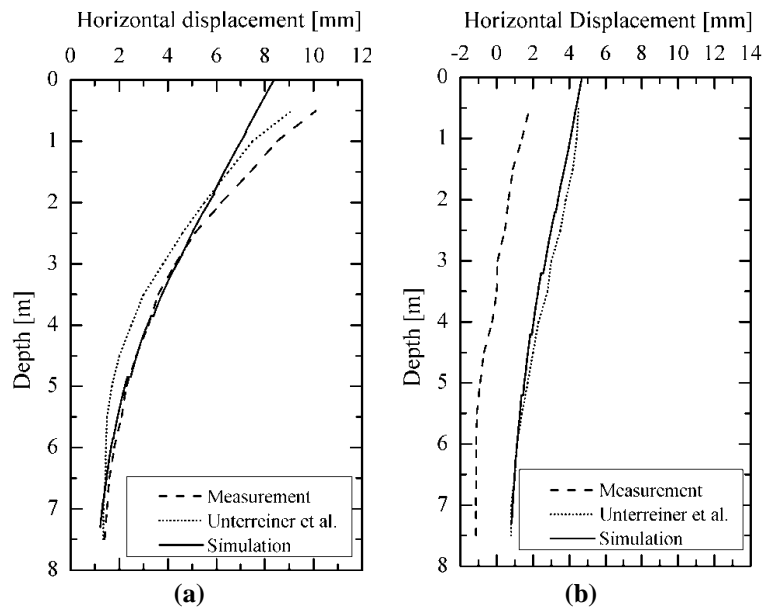
Fig. 5. Comparison of the predicted horizontal displacements in the backfill with measured results in phase 5 at: a) 2 m; b) 4 m; and c) 8 m behind the wall facing
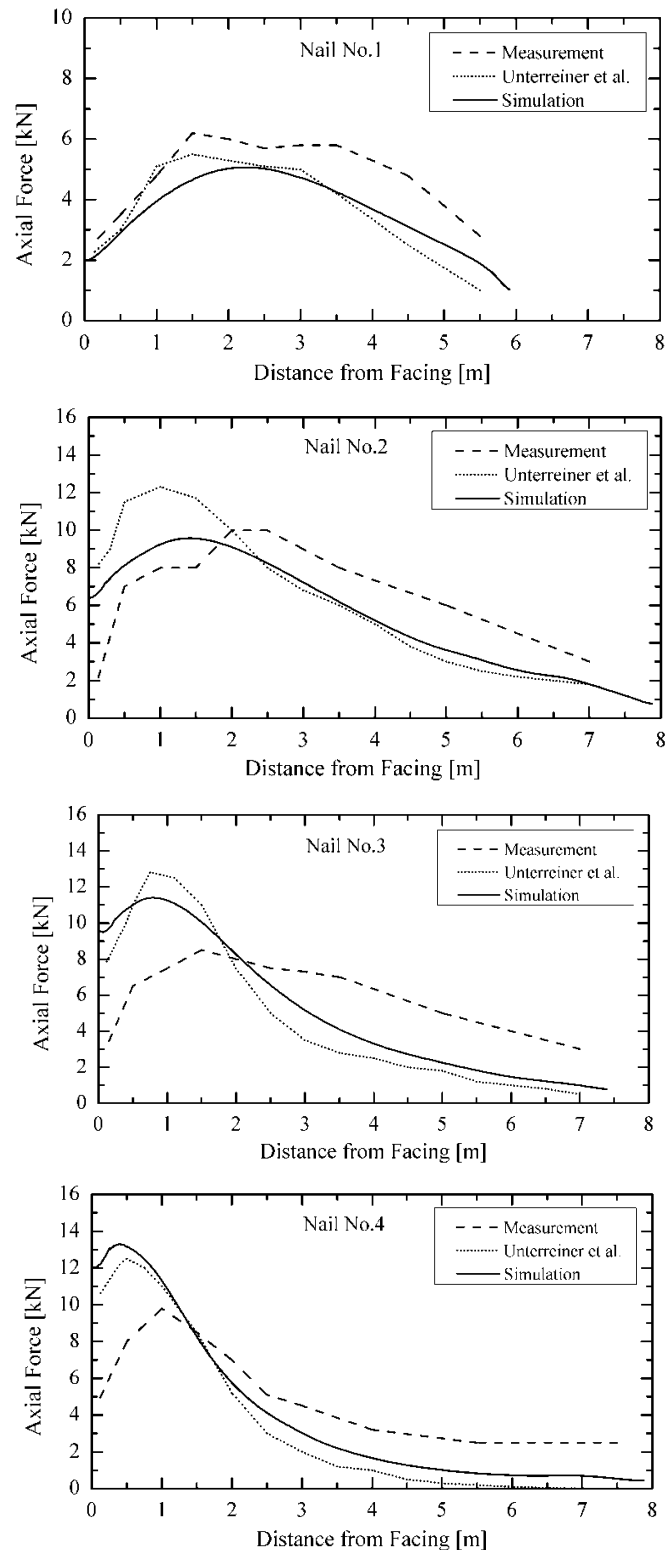
Fig. 6. Tensile force distribution in the nails at the end of phase 5

3. Parametric Analysis on the Nailing Pattern

The nails length can be considered constant in the height of the wall. This approach may not be the best design if the wall deformation is taken into account. To study the effect of nailing pattern on the performance of nailed wall, nine patterns were considered (Figure 7). The nails length in pattern (a) is uniform and equal. In patterns (b) and (c), half and two-thirds of nails are uniformly long nails, respectively and the other nails are short nails. In

patterns (d) and (e), the length of each 3 or 2 nails are linearly decreased from the maximum nail length at the top of the wall to the minimum nail length at the bottom of the wall, respectively. The ratio of length of the shortest nail to the longest nail has been considered 0.5 and 0.7 in all variable patterns.

In addition to the nailing pattern, the other factors which have effect on the wall deformation are nails spacing, wall height and surcharge load. The considered values for these parameters are presented in Table 5. So, parametric analysis was conducted to determine the effects of these parameters on the wall deformation with various nailing layouts.

Figure 8 shows the typical geometry of the wall used for the parametric analysis. These dimensions are chosen in such a way that minimizes the effects of boundary conditions on simulation results. The stability of nailed walls was analyzed using the limit equilibrium method. The overall stability of all patterns has been analyzed according to the recommended procedure and safety factors in the nailing manual of FHWA (Lazarte et al., 2015) for temporary condition. The objective of limit equilibrium analysis was determination of nails length in such a way that all models have the same safety factor of overall stability equal to 1.35.

The diameter of nail bar has been considered 32 and 40 mm for the 12 and 18 m walls, respectively. The nail bar is surrounded by 10 cm cement grout. The nail orientation relative to horizontal plane is 15 deg. The thickness of shotcrete facing is 10 cm. The properties of nail and shotcrete used in the parametric analysis are shown in Tables 6 and 7.

Table 8 shows the soil properties used in the parametric analysis. These parameters are matching with the properties of dense clayey sand and gravel soils. The hardening soil model was used to simulate the stress-strain behavior of soil.

After creating geometry of the model, defining material properties and mesh generation, the initial condition of stress and stage construction should be defined. Each stage construction involved two phases: excavation with 2 m height and activation of nail and shotcrete elements. This process has been continued until reaching to base of the wall.

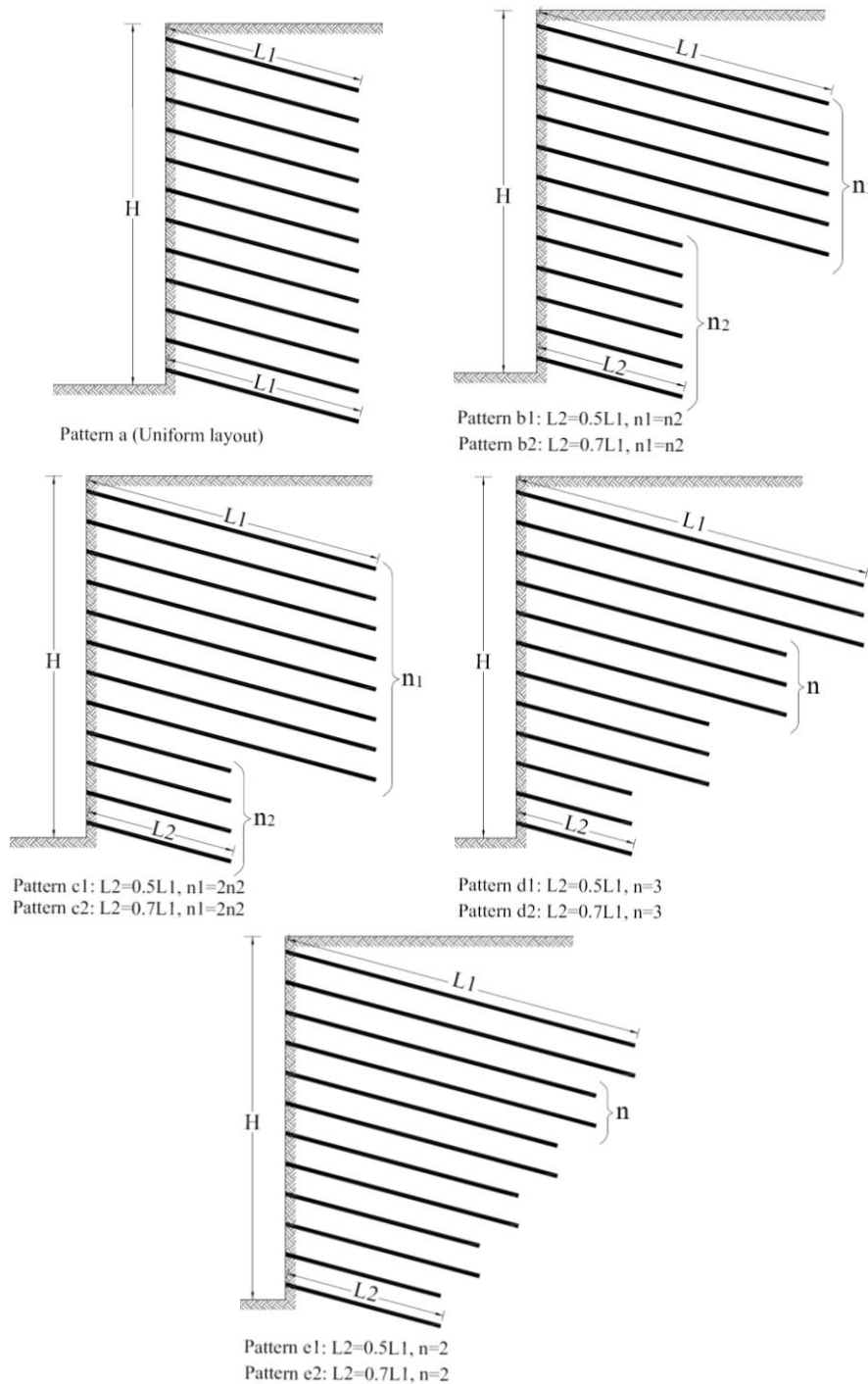**Table 5.** Variable parameters in parametric analysis

Parameter	Symbol	Unit	Values
Wall height	H	m	12, 18
Surcharge	q	kPa	0, 50
Nails spacing	$S_h = S_v$	m	1.5, 2

Table 6. Properties of nails used for the parametric analysis

Parameter	Symbol	Unit	H=12 m	H=18 m
Diameter	φ	mm	32	40
Yield force	F_y	kN	320	500
Bond diameter	d	m	0.1	0.1
Bond skin friction	α	kPa	200	200
Axial stiffness	EA	kN	3.17×10^5	4.93×10^5
Poisson ratio	ν	-	0.2	0.2

Table 7. Properties of shotcrete facing used for the parametric analysis

Parameter	Symbol	Unit	Value
Unit weight	γ	kN/m^3	24
Young's modulus	E	kPa	21×10^6
Axial stiffness	EA	kN/m	2.1×10^6
Bending stiffness	EI	kN.m^2/m	1750
Shotcrete thickness	d	cm	10
Poisson ratio	ν	-	0.2

Pattern a (Uniform layout)

Pattern b1: L2=0.5L1, n1=n2
Pattern b2: L2=0.7L1, n1=n2

Pattern c1: L2=0.5L1, n1=2n2
Pattern c2: L2=0.7L1, n1=2n2

Pattern d1: L2=0.5L1, n=3
Pattern d2: L2=0.7L1, n=3

Pattern e1: L2=0.5L1, n=2
Pattern e2: L2=0.7L1, n=2

Fig. 7. Nailing patterns for parametric analysis

Table 8. Soil properties used in the parametric analysis

Parameter	Symbol	Unit	Value
Cohesion	c	kPa	30
Friction angle	φ	deg	36
Dilation angle	ψ	deg	6
Unit weight	γ	kPa	20
Reference loading stiffness	E_{50}^{ref}	kPa	7.0×10^4
Reference oedometer loading stiffness	E_{oed}^{ref}	kPa	7.0×10^4
Reference unloading stiffness	E_{ur}^{ref}	kPa	2.1×10^5
Reference confining pressure	P^{ref}	kPa	100
Poisson ratio	ν	-	0.3
Fabric parameter	m	-	0.5
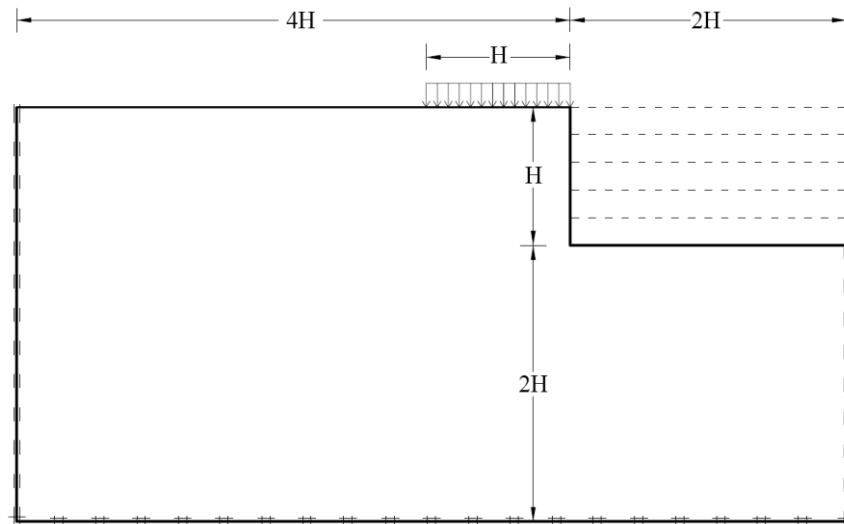
Fig. 8. Geometry of nailed walls used for the parametric study

4. Results and Discussion

4.1. Density of Nails

In Figure 9, the normalized maximum nail lengths for various patterns are presented. Also, nail density per unit area of wall facing for the various patterns is shown in Figure 10. The density of nail is defined as follows:

$$Nail\ density = \frac{\sum L_{nail}}{S_h \times H} \tag{7}$$

where $\sum L_{nail}$: is the summation of all nails length in a vertical row, S_h: is the horizontal spacing of the nails and H: is the wall height.

As observed in Figure 9, pattern (a) has the minimum nail length and patterns (b1), (d1) and (e1) has the maximum nail length. The maximum nail length of the patterns 2 (in which $L_2 = 0.7L_1$) are less than patterns 1 (in which $L_2 = 0.5L_1$). The results of analyses indicate that by increasing the nail spacing to 2 m, the nails length increases. As seen in Figure 9, the normalized nails length increases by increasing the height of wall and surcharge load.

As it is observed in Figure 10, the nailing pattern has minor influence on the nail density and its variation is between 5 to 15 percent. However, nails spacing has considerable effect on nail density. By increasing the nail spacing from 1.5 m to 2

m, the nail density decreases about 20 to 40 percent. This indicates that despite of the increasing of the maximum nail length, the nail density decreases by increasing of nails spacing. In fact, by increasing the spacing of nails from 1.5 m to 2 m, the effective area of each nail increases from 2.25 to 4 m^2, i.e. 78 percent. However, the length of the nails does not increase with this ratio according to the Figure 10. As a result, increasing the nail spacing will reduce the density of nail and optimize the design of soil-nailed wall economically. Also, the nail density increases considerably by increasing the height of the wall and surcharge load.

4.2. Deformations of Nailed Walls

The results of deformation analysis are presented in Figures 11 and 12 in the form of normalized deformations at the top of the wall (δ_h/H and δ_v/H). As can be seen in these figures, the deformations of uniform pattern in various conditions are significantly greater than that of the variable patterns. Among the variable patterns, patterns 1 have relatively less deformation than patterns 2. Also, it can be seen that the patterns (d1) and (e1) in most cases have the least deformations in comparison to other variable patterns.

As mentioned above, the nail density in uniform and variable patterns is approximately equal. Thus, it can be concluded that these observations are

related to the maximum length of the nail in the upper rows. The patterns in which the nails lengths are more variable, the length of the upper nails should be increased to provide the required safety factor of stability. Increasing the nails length in the upper rows will cause more constraint for the wall and reduce deformations, especially horizontal deformations.
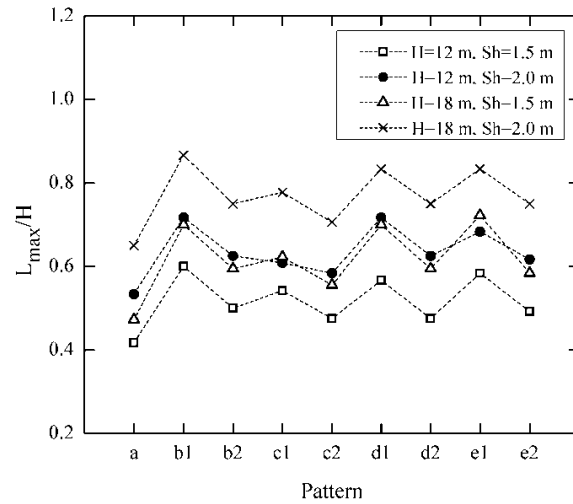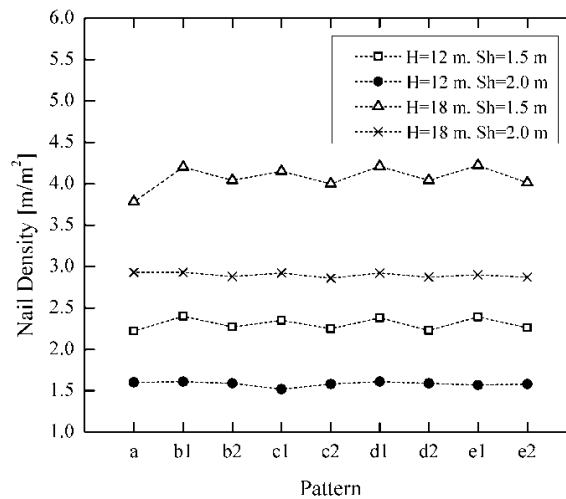

(a)
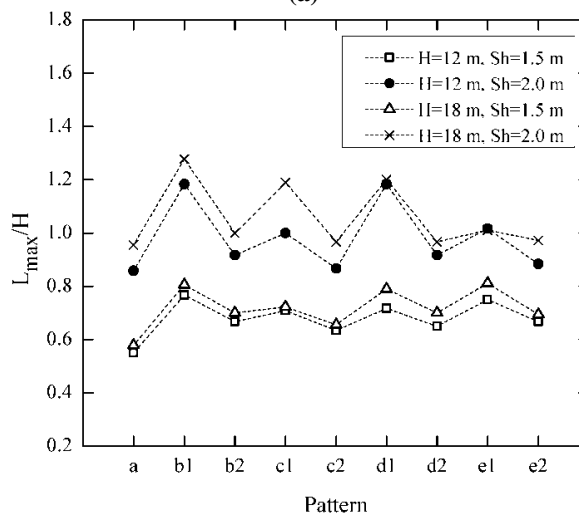
(b)

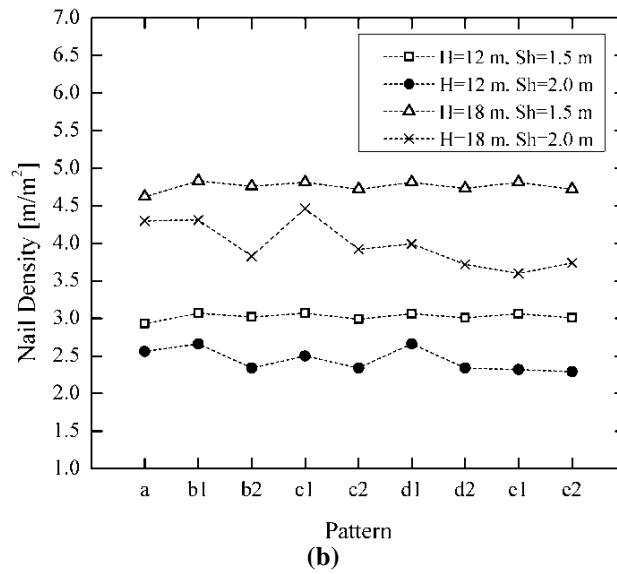**Fig. 9.** Maximum length of nails for different patterns: a) q = 0 kPa; and b) q = 50 kPa

(a)

(b)

Fig. 10. Nail density for different patterns: a) q = 0 kPa; and b) q = 50 kPa
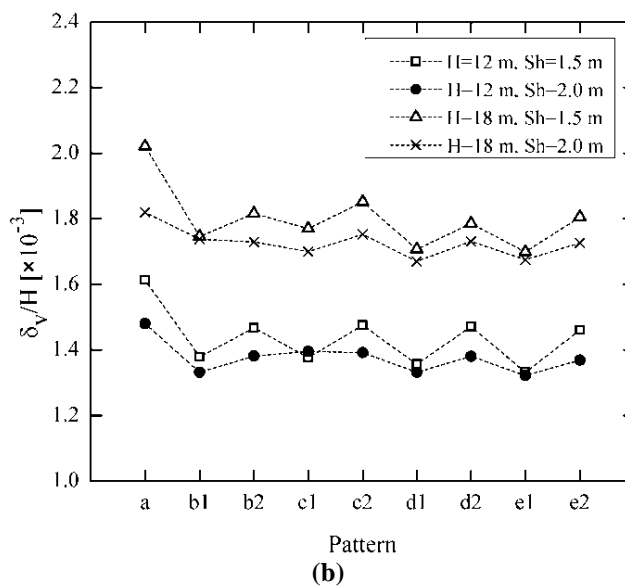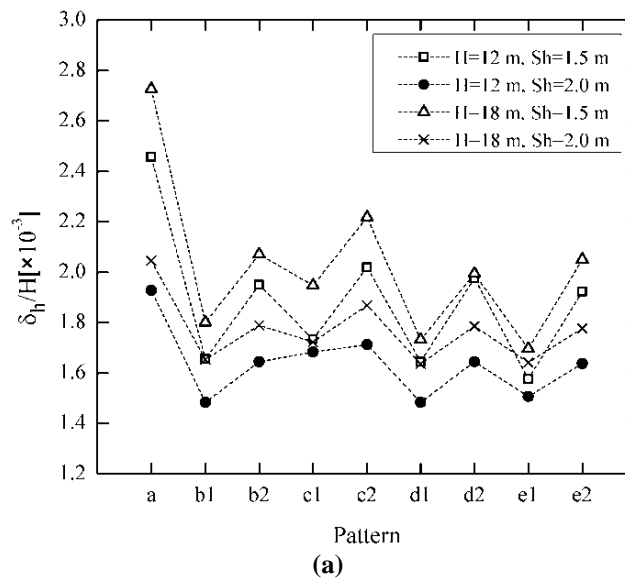

(a)

(b)

Fig. 11. Normalized maximum wall deformation for different patterns (q = 0 kPa): a) Horizontal displacement; and b) Vertical displacement

As stated, the nailed walls were designed based on the FHWA manual and the target safety factor of stability in all of walls is the same. This implies that the nails length should be increased by increasing of nails spacing. Regarding the nails spacing, important point that can be seen in Figures 11 and 12 is that the wall deformation is reduced by increasing the spacing of nails which is directly related to the long nails in the sparse layouts. In this case, it should be noted that although the maximum length of the nail increases, the density of nails per unit area of wall facing decreases. Therefore, it can be concluded that the length of the upper nails is more effective than the nail density on reducing deformation. However, these two factors are more effective on horizontal displacement of the wall and in the case of vertical displacement; they balance the effects of each other. Consequently, the amount of the settlement has not changed much by changing the nails spacing.

In Figure 13, the horizontal deformation at the top of the wall is plotted versus the maximum nail length for all analyses. These two parameters were normalized in terms of the height of wall, so that all of the results can be presented in one graph for various heights of the wall. This plot shows the effect of the maximum length of the nails on the horizontal displacement of the nailed wall more accurately. The general trend of data in this figure indicates that with increasing the maximum length of the nails, the horizontal deformation of the wall decreases.

Regarding the above discussions, it can be concluded that the optimal pattern for reducing the nailed wall deflections is that the long nails should be installed at the top of the wall and nails length reduced in the wall height. The linear reduction of the nails length at the wall height (for example pattern e1) can be considered as an optimal pattern, because the nails length changes according to the slip surface inclination. Also, designing of nailed wall with the greater nails spacing leads to reduction of

wall deformation and optimal economical design.

4.3. Damage Severity

There are various criteria for assessing the effects of excavation-induced ground movements on the performance and serviceability of the adjacent buildings. One of the most famous criteria for this purpose is angular distortion criterion that is proposed by Boscardin and Cording (1989). Boscardin and Cording (1989) considered both vertical and horizontal ground deformations for evaluating the damage of adjacent structures due to excavation-induced ground movements. As can be seen in Figure 14, the severity of damages is divided into four zones based on horizontal extension strain and angular distortion, namely Negligible damage (NEGL.), Very slight damage (V.SL.), Slight damage, and Moderate to Severe damage. The horizontal extension strain (ε_v) and angular distortion (β) are defined as follows:

$$\beta = (\delta_{v1} - \delta_{v2})/L \qquad (8a)$$
$$\varepsilon_h = (\delta_{h1} - \delta_{h2})/L \qquad (8b)$$

where L: is the length of adjacent structure, and δ_v and δ_h: are the vertical and horizontal displacement at two edges of structure, respectively.

It should be noted that the ground movements at the ground surface on the top of the wall varies non-linearly with the distance from the wall edge. In the vicinity of the nailed wall, the rate of variations is greater, and by increasing the distances from the wall, deformation values and their rate of variation are reduced. Therefore, there are various values of horizontal extension strain and angular distortion by changing the distance from the wall. In order to consider the proper estimation for L in the above equations, the influence zone of excavation should be considered that depends on various conditions such as soil type and excavation depth. The results of the analyses indicate that the main effects of excavation usually occur at a distance equal

to the height of the wall. Therefore, to obtain the proper values for the horizontal strain and angular momentum parameters, the rate of variation of the deformation at the distance of H from the wall edge was used.
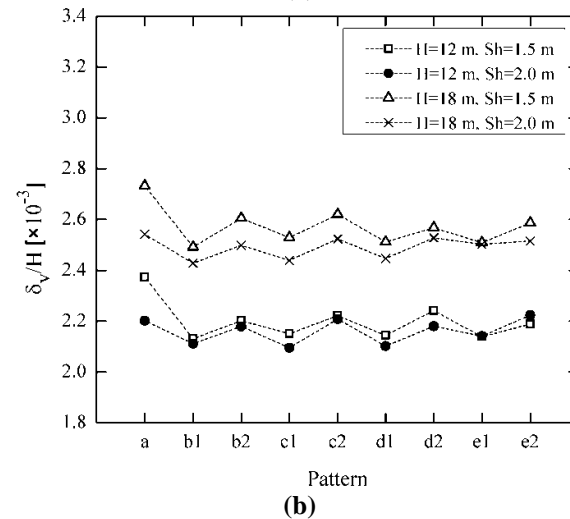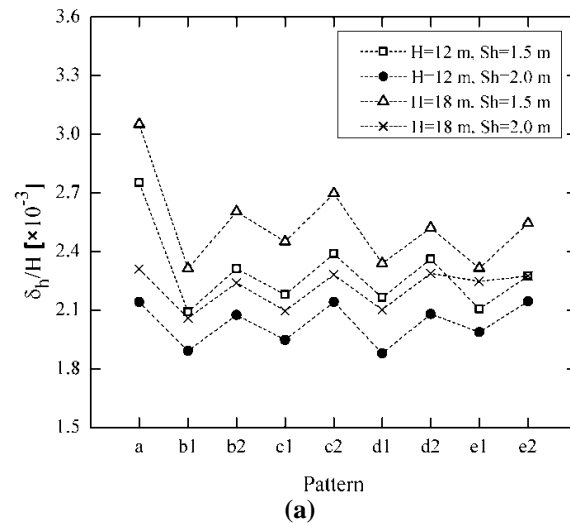
Fig. 12. Normalized maximum wall deformation for different patterns (q = 50 kPa): a) Horizontal displacement; and b) Vertical displacement
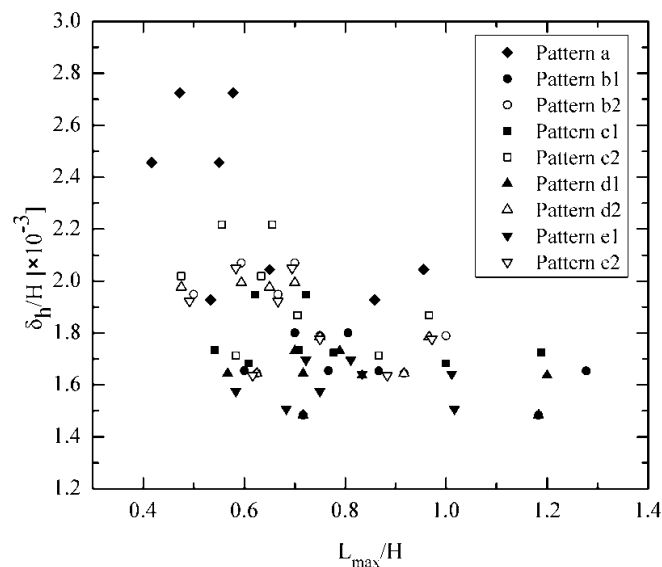
Fig. 13. Relationship between maximum horizontal displacement and maximum length of nails for different patterns
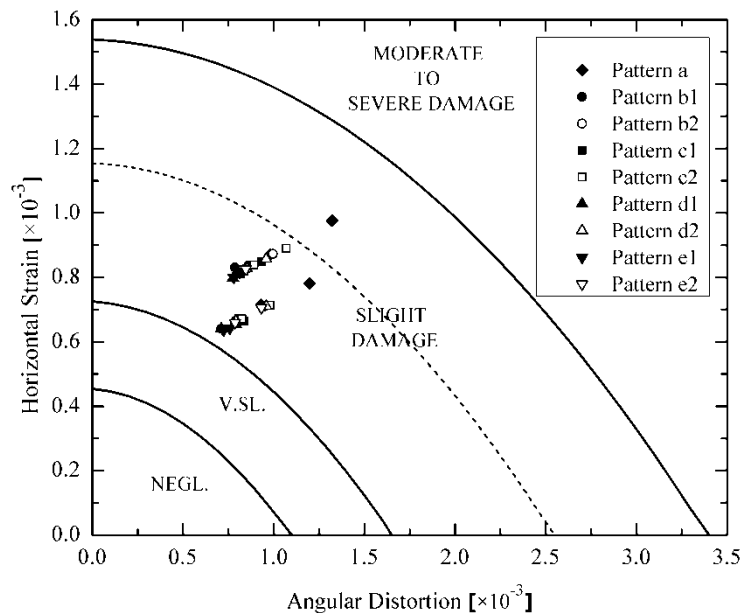
Fig. 14. Relationship between angular distortion and horizontal strain for damage category (q = 0 kPa)

In Figures 14 and 15 the values of the horizontal extension strain and the angular distortion for all the models were plotted in the Boscardin and Cording graph. Figures 14 and 15 are related to the models without surcharge and with surcharge of 50 kPa, respectively. As seen, in case of no surcharge (q = 0), the severities of displacements are located in the lower half of slight damage region while in the presence of surcharge they are located in the upper half of the slight damage region. As shown in these figures the severity of damages in the uniform patterns are more than variable ones. Even in Figure 15, one point is located in moderate to severe damage region. This point is related to the uniform pattern with the wall height of 18 m and the nails spacing of 1.5 m.

These graphs assist in considering the appropriate safety factor to achieve the allowable displacement. As seen in Figure 14, in the case of no surcharge, the excavation-induced displacements can be considered allowable. Specially, by taking into account the recommendations of the previous section (using the variable patterns and increasing the length of upper nails), it is possible to reduce deformations up to very slight damage region. Therefore, considering the stability safety factor equal to 1.35 can be appropriate in the case of no

surcharge. But as seen in Figure 15, the existence of surcharge increases the wall deformations. On the other hand, due to the presence of the structure in the vicinity of the wall, the allowable deformations are less than the no surcharge case. Therefore, the safety factor equal to 1.35 is not a good criterion for design of nailed walls adjacent to the structures.

In order to investigate the deformations of nailed walls with different safety factors of stability, the optimal case in the previous section (Pattern e1 and nails spacing of 2 m) was considered and the nailed wall was designed considering different safety factors of stability. The wall height of 18 m and 50 kPa surcharge were considered. Afterwards, the wall deformations were calculated using finite element analysis and the amount of horizontal strains and angular distortions were plotted on the Boscardin and Cording (1989) graph and its distance from the boundary of the very slight damage (V.SL.) region were measured. In Figure 16, the method of calculation is schematically shown.

The variation of distance from the V.SL. boundary versus safety factor of stability is shown in Figure 17. As seen, the deformations reduce by increasing the safety factor and approach to the V.SL. boundary. It can be concluded from this

graphs that the deformations of nailed walls with surcharge will be located in the V.SL. region if the safety factor of stability is considered greater than 1.5. These deformations can be acceptable for the ordinary structures. It should be noted that this conclusion is depended on the various conditions such as soil type, the height of the wall, and the amount of the surcharge load. So, the permissible deformations cannot be guaranteed by taking into account only the proposed safety factor and deformation analysis is necessary. The proposed safety factor can be considered as a preliminary guide for design of optimal and safe soil nailed walls in the urban areas.
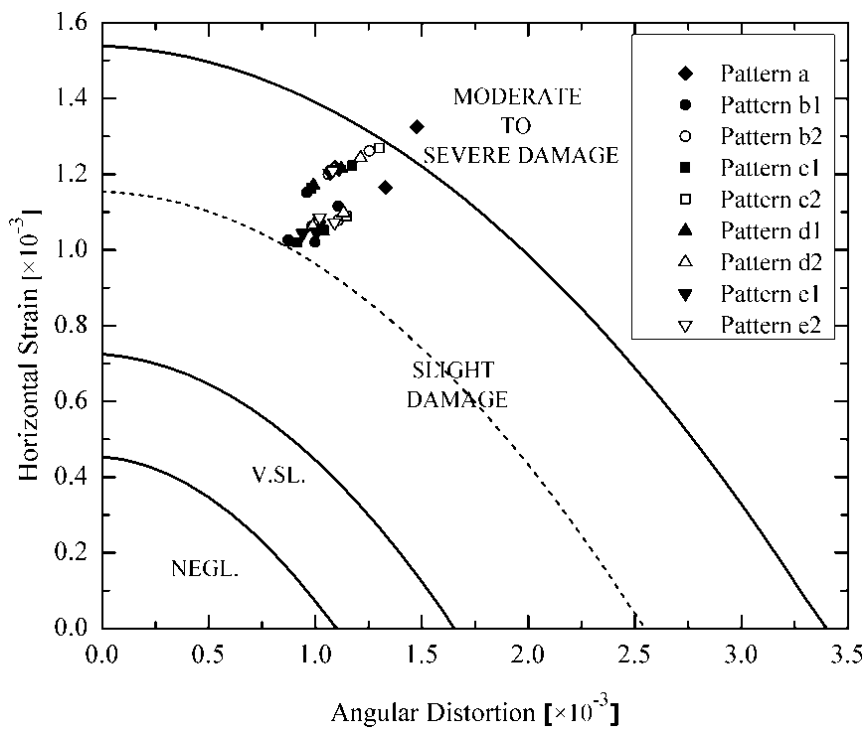

Fig. 15. Relationship between angular distortion and horizontal strain for damage category (q = 50 kPa)
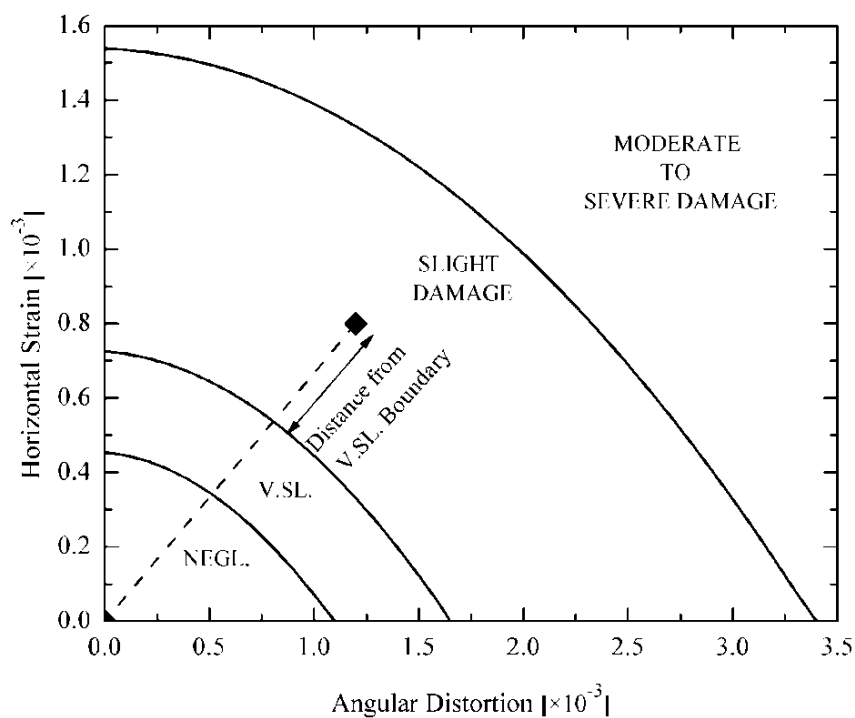

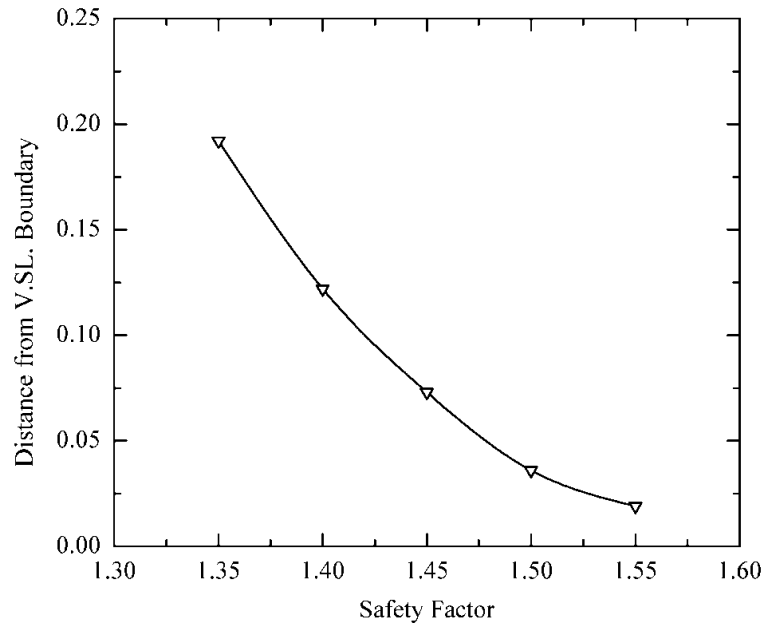**Fig. 16.** Definition of distance from the boundary of the V.SL. region

Fig. 17. The variation of distance from the V.SL. boundary versus safety factor

5. Conclusions

In this study, the effects of the nailing pattern on the wall deformation were studied using the non-linear finite element analysis. Major results concluded from this study are summarized as follow:

- The nailing pattern has minor influence on the nail density. It can be indicated that this conclusion is related to the maximum length of the nail in the upper rows. The patterns in which the nails lengths are more variable, the length of the upper nails should be increased to provide the required safety factor of stability.
- Nails spacing has considerable effect on the nail density. This indicates that despite of the increasing of the maximum nail length, the nail density decreases by increasing of nails spacing. As a result, increasing the nail spacing will reduce the density of nail and optimize the design of nailed wall.
- The deformations of uniform pattern in various conditions are significantly greater than that of the variable patterns. The simulation results indicate that using the variable pattern with long nails at the top of the wall reduces the lateral deformation and the density of nails of

soil nailed wall. Increasing the nails length in the upper rows will cause more constraint for the wall and reduce deformations, especially horizontal deformations.

- To achieve the optimal nailing pattern for reducing the nailed wall deflections, the long nails should be installed at the top of the wall and nails length should be reduced in the wall height. The linear reduction of the nails length at the wall height (for example pattern e1) can be considered as an optimal pattern.
- Based on the angular distortion criterion that is proposed by Boscardin and Cording (1989), the severity of damages in the uniform patterns are more than variable ones.
- Deformation analysis of optimal pattern in this study with different safety factors of stability indicated that considering the stability safety factor equal to 1.35 can be appropriate in the case of no surcharge. However, it is not a good criterion for design of nailed walls adjacent to the structures. The minimum safety factor of 1.5 can be considered as a preliminary guide for design of optimal and safe soil nailed walls in the urban areas.

6. Acknowledgment

7. References

Abbas, H., El Sherbiny, R. and Salam, A. (2020). "Numerical analysis of soil nail walls in hybrid retaining wall systems", *Geo-Congress 2020*, Minneapolis, Minnesota.

Ardakani, A., Bayat, M. and Javanmard, M. (2014). "Numerical modeling of soil nail walls considering Mohr Coulomb, hardening soil and hardening soil with small-strain stiffness effect models", *Geomechanics and Engineering*, 6(4), 391-401.

Boscardin, M.D. and Cording, E.G. (1989). "Building response to excavation-induced settlement", *Journal of Geotechnical Engineering*, ASCE, 115(1), 1-21.

Chu, L.M. and Yin, J.H. (2005). "Comparison of interface shear strength of soil nails measured by both direct shear box tests and pull-out tests", *Journal of Geotechnical and Geoenvironmental Engineering,* ASCE, 131(9), 1097-1107.

Dupla, J.C. and Canou J. (1994). "Caractérisation mécanique du sable de Fontainebleau à partir d'essais triaxiaux de compression et d'extension", Rapport Interne Clouterre II, CERMES–ENPC.

FHWA (1993). "Recommendations Clouterre 1991 (English translation): Soil nailing recommendations", Report No. FHWA-SA-93-026, Federal Highway Administration, Washington, D.C.

Fan, C.C., and Luo, J.H. (2008). "Numerical study on the optimum layout of soil-nailed slopes", *Computers and Geotechnics*, 35(4), 585-599.

Gharedaghi, H. and Shahir, H. (2019). "Parametric assessment of lateral pressure on piles and laggings in an anchorage system", *Journal of Geoengineering*, 14(1), 11-20.

Hajiazizi, M. and Mirzazadeh, Z. (2020). "Determination of creep-induced displacement of soil slopes based on LEM", *Civil Engineering Infrastructures Journal*, 53(2), 341-358.

Halabian, A.M., Sheikhbahaei, A.M. and Hashemolhosseini, S.H. (2012). "Three dimensional finite difference analysis of soil-nailed walls under static conditions", *Geomechanics and Geoengineering*, 7(3), 183-196.

Hitha, S., Vijayshree, S., Animesh, S. and Ramkrishnan, R. (2019). "Regression analysis of soil nailing parameters using finite element and limit equilibrium methods", *Australian Geomechanics Journal*, 54(3), 137-147.

Lazarte, C.A., Robinson, H., Gómez, J.E., Baxter, A., Cadden, A. and Berg, R. (2015). "Geotechnical engineering circular No. 7: Soil nail walls - Reference manual", Report No. FHWA-NHI-14-007, National Highway Institute, US Department of Transportation, Federal Highway Administration, Washington D.C.

Liu, J., Shang, K. and Wu, X. (2016). "Stability analysis and performance of soil-nailing retaining system of excavation during construction period", *Journal of Performance of Constructed Facilities*, ASCE, 30(1), C4014002.

Moniuddin, Md. K., Manjularani, P, and Govindaraju, L. (2016). "Seismic analysis of soil nail performance in deep excavation", *International Journal of Geo-Engineering*, 7(1), 1-10.

Plumelle, C., Schlosser, F., Delage, P. and Knochenmus, G. (1990). "French national research project on soil nailing: Clouterre", *Proceedings of Conference of Design and Performance of Earth Retaining Structures,* ASCE Geotechnical Special Publications No. 25, 660-675.

Rashidi, F., Shahir, H. and Arefizade, H. (2019). "Comparative study of anchored wall performance with two facing designs", *Civil Engineering Infrastructures Journal*, 52(1), 23-40.

Rashidi, F. and Shahir, H. (2019). "Numerical investigation of anchored soldier pile wall performance in the presence of surcharge", *International Journal of Geotechnical Engineering*, 13(2), 162-171.

Rawat, S. and Gupta, A.K. (2016). "Analysis of a nailed soil slope using limit equilibrium and finite element methods", *International Journal of Geosynthetics and Ground Engineering*, 2(4), 1-23.

Schanz, T. and Vermeer, P.A. (1998). "On the stiffness of sand", In: *Pre-Failure Deformation Behaviour of Geomaterials*, London, 383-387.

Schlosser, F., Unterreiner, P. and Plumelle, C. (1993). "Validation des méthodes de calcul de clouage par les expérimentations du projet national Clouterre", *Revue Française de Géotechnique,* 64, 11-20.

Seo, H.J., Lee, I.M. and Lee, S.W. (2014). "Optimization of soil nailing design considering three failure modes", *KSCE Journal of Civil Engineering*, 18(2), 488-496.

Sharma, A. and Ramkrishnan, R. (2020). "Parametric optimization and multi-regression analysis for soil nailing using numerical approaches", *Geotechnical and Geological Engineering*, 38, 3505-3523.

Tei, K., Taylor N.R. and Milligan G.W.E. (1998). "Centrifuge model tests of nailed soil slopes", *Soils and Foundations*, Japanese Geotechnical

Society, 38(2), 165-177.

Unterreiner, P., Benhamida, B. and Schlosser, F. (1997). "Finite element modeling of the construction of a full scale experimental soil-nailed wall", *French National Research Project Clouterre-Ground Improvement,* 1(1), 1-8.

Yang, M.Z. and Drumm, E.C. (2000). "Numerical analysis of the load transfer and deformation in a soil nailed slope", In: *Numerical Methods in Geotechnical Engineering,* pp. 102-115.

Zhang, M., Song, E. and Chen, Z. (1999). "Ground movement analysis of soil nailing construction by three-dimensional (3-D) finite element modeling (FEM)", *Computers and Geotechnics*, 25(4), 191-204.